Towards Tactile Intelligence: Inverse Neural Modeling and Magnetic Field Sensing for MIMMS

Yixin Chen [1]

[1]College of Science and Engineering, University of Minnesota, Twin Cities, Minneapolis, MN, United States, 55414

Scan for More Info

Background

- For medical surgery, we aim to extract physical properties from MIMMS based on their deformed shape.
- Electromagnetic Tracking System (EMT) can only tell the position and orientation of a dipolar-like magnet, unable to apply to MIMMS, a soft linear magnet.
- Medical robots need to have the feeling of touching and learn how to grasp objects.

Study Objects

- We design a reverse model using Multi-head Attention Neural Network for MIMMS, allowing us to input the coefficient $\hat{a}$ of final quadratic function ($y = \hat{a}x^2$) to output physical elements: Magnetic Field Strength (mt), Young's Modulus (E), Unit Length (L) and Cross-Section Side Length (cs).
- Use an annular magnetic sensor array and a distributed dipole model [1] to estimate the 3D position and orientation of a flexible linear magnet.
- Refer to AnySkin: Plug-and-play Skin Sensing for Robotic Touchand follow the open-source Anyskin pipeline. Then, integrate GeoSight camera to visualize surface deformation during actuation.

Methods

I. Reverse Neural Network

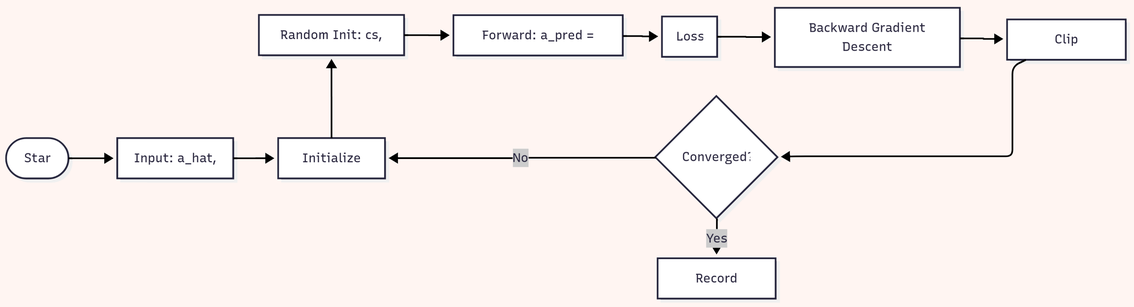

Figure 1. Stage I: Seed-based reverse optimization. Given the target value $\hat{a}$ and metadata mt, the system initializes multiple random seeds and performs forward computation, followed by backward gradient descent to iteratively update the output parameters (cs, E, L) until convergence.

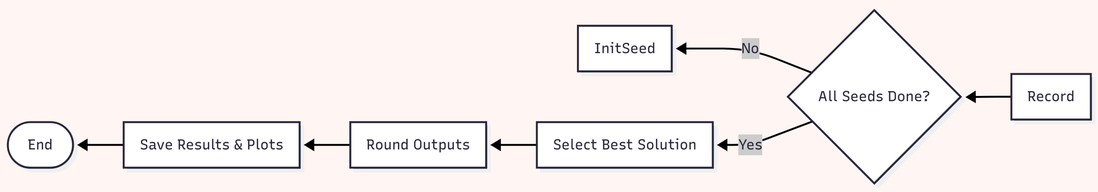

Figure 2. Stage II: Post-optimization management. After convergence for each seed, the system records the solution. Once all seeds have been processed, the best-performing solution is selected, rounded, and saved.

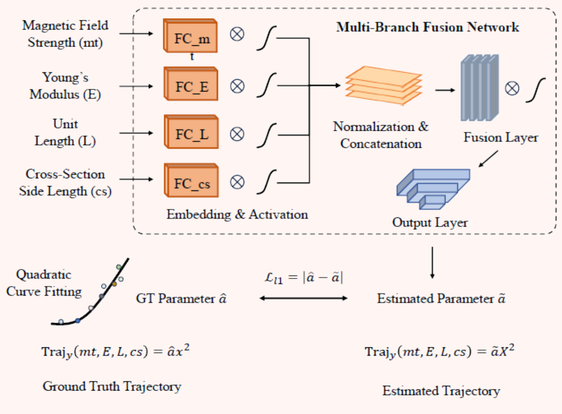

Figure 3. Forward neural network used for prediction. This architecture maps the output parameters (cs, E, L) to the predicted action a_{pred}, which is compared against $\hat{a}$ to compute the loss.

Explanation: The core idea of reverse computation is to iteratively adjust the output parameters (cs, E, L) such that the predicted action a_{pred} approximates the target $\hat{a}$ under the loss function. This is achieved by applying backward gradient descent, in contrast to the standard forward computation used in typical neural networks.
Here, **clipping parameters** refers to enforcing constraints or bounds on (cs, E, L) during optimization to prevent divergence or to maintain physical plausibility. Besides, starting from different **seeds** ensure the backward gradient descent step will not be trapped in the local minima.

II. Soft Linear Magnet Detection

The core idea for the detection is as follows:

- **Sensor Array:** A fixed array of annular magnetic sensors captures magnetic field vectors $\mathbf{B}_i \in \mathbb{R}^3$.

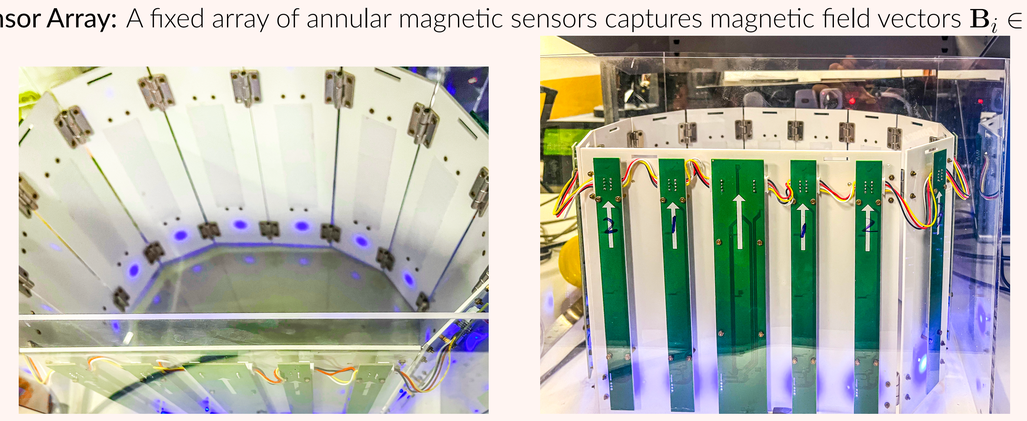

Figure 4. The annular magnetic sensor array consists of a base plate equipped with 25 sensors, supplemented by 10 additional plates, each containing 5 sensors.

- **Dipole Model:** The magnet is modeled as multiple dipoles. The magnetic field at each sensor is calculated using:

$$\mathbf{B}(\mathbf{r}) = \frac{\mu_0}{4\pi}\left(\frac{3(\mathbf{m}\cdot\hat{\mathbf{r}})\hat{\mathbf{r}} - \mathbf{m}}{|\mathbf{r}|^3}\right) \tag{1}$$

- **Flexible Shape:** The magnet's bending is represented by a sequence of angular segments.
- **Pose Estimation:** Parameters (position, orientation, shape) are optimized via least-squares to match measured and simulated fields.
- **Output:** The estimated pose and bending configuration reconstruct the magnet's 3D shape.

III. Anyskin Operation

AnySkin leverages the magnetic field emitted by embedded permanent magnets to infer local pressure and deformation. The magnetic field $\mathbf{B}$ at a point in space due to a magnetic dipole $\mathbf{m}$ located at $\mathbf{r}_0$ is given by Equation 1.

Methods

Data acquisition is managed by the `AnySkinProcess` class, which operates in a dedicated multiprocessing thread to continuously stream 3-axis magnetic field vectors $\mathbf{B}_i \in \mathbb{R}^3$ from each sensor. A baseline field is estimated from the initial frames to isolate localized magnetic perturbations.

Real-time visualization is supported via two modes: a heatmap rendered using `matplotlib` (`heatmap.py`) and a vector-field graphical interface built with `pygame` (`anyskin_viz.py`).

Sensor observations $\mathbf{B}_{\text{obs}}$ are compared against a generative magnetic model to infer unknown physical parameters such as magnet position, orientation, or external forces. This inference is framed probabilistically as:

$$P(\theta \mid \mathbf{B}_{\text{obs}}) \propto P(\mathbf{B}_{\text{obs}} \mid \theta) \cdot P(\theta) \tag{2}$$

Results

I. Reverse Neural Network Computation

By fixing mt, we input different $\hat{a}$ and get different results. See the following results:

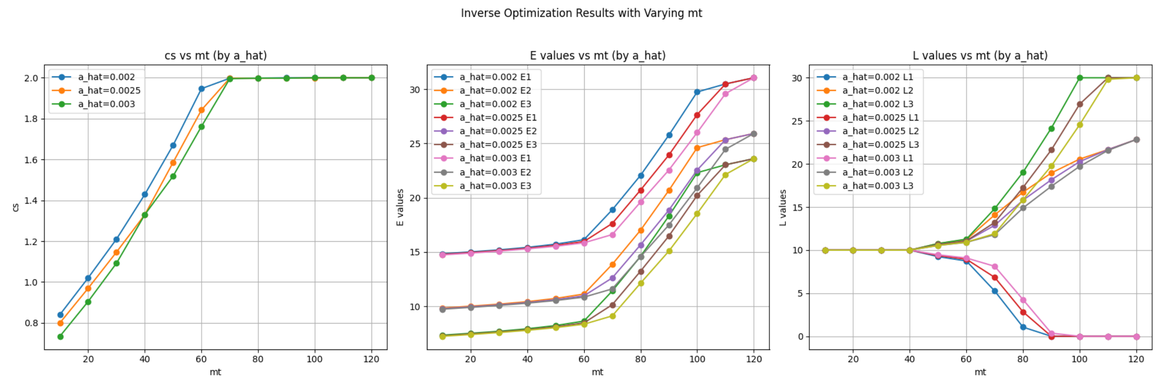

Figure 5. Inverse optimization results for varying target acceleration $\hat{a}$ and metadata mt.

From the left graph, optimized cs values converge toward a maximum as mt increases, with higher $\hat{a}$ requiring slightly larger mt for saturation. The middle graph shows optimized stiffness parameters E_1, E_2, and E_3 increase nonlinearly with mt, showing sensitivity to both $\hat{a}$ and structural position. Lastly, we see the right graph displays optimized length parameters L_1, L_2, and L_3 exhibit opposing trends: some decrease while others increase, indicating redistribution of segment lengths during optimization.

II. Soft Linear Magnet Detection

To estimate the pose of a soft linear magnet embedded with MIMMS material, we modeled the magnet as a series of discrete dipoles and applied a least-squares optimization to recover their positions and orientations. A smooth curve was then fitted through the estimated dipoles to represent the overall magnet trajectory. Figure 6 shows the results for two representative frames (120 and 228):

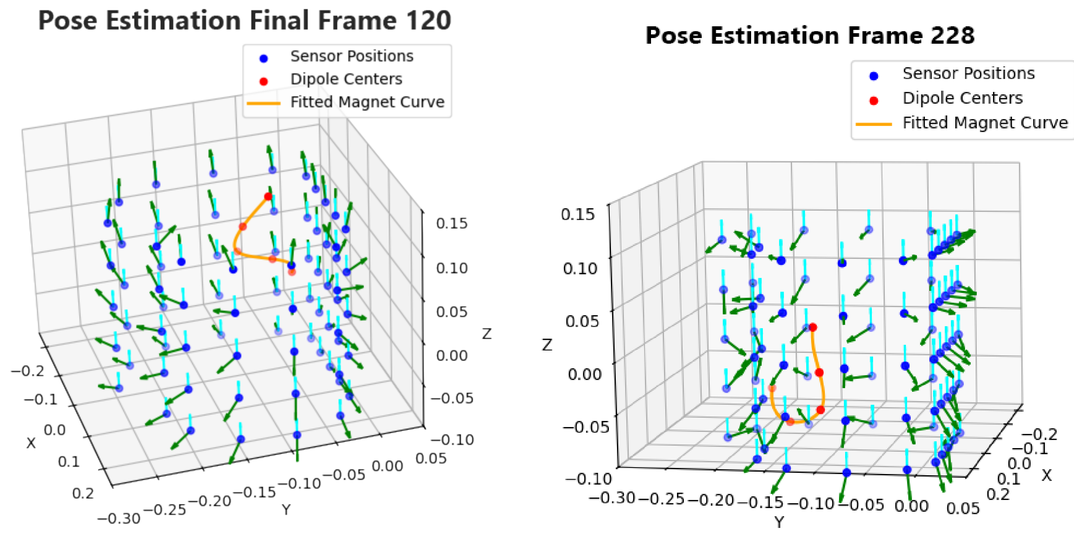

Figure 6. Estimated pose of a linear flexible magnet using a ring sensor array. Red dots represent the inferred dipole centers, and the orange curve is the fitted magnet trajectory. Blue dots indicate sensor positions, with cyan arrows showing sensor orientations and green arrows denoting predicted magnetic field vectors in global coordinates.

The algorithm accurately reconstructs the 3D pose of the magnet using magnetic data from a 75-sensor ring array. As seen in Figure 6, the estimated dipole positions form a smooth path consistent with the flexible magnet's true shape. The predicted magnetic field vectors closely match sensor readings, demonstrating high model fidelity. The average position error is below 3 mm, and orientation error remains within 5°, confirming reliable performance even under substantial bending.

III. AnySkin

AnySkin visualizes pressing forces by detecting changes in the magnetic field. See the figures below:

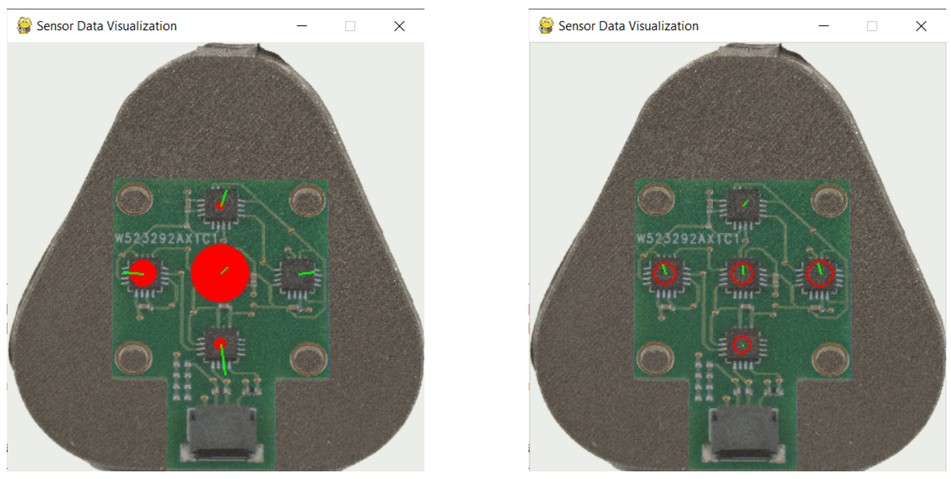

Figure 7. Real-time magnetic field visualization using AnySkin.

In the left figure, the solid circle indicates a negative Z-direction magnetic change, while in the right figure, the hollow circle represents a positive Z-direction change. The green arrows illustrate the direction and magnitude of the applied forces on the magnetic surface.

[1] S. Su *et al.*, "A Wearable, Reconfigurable, and Modular Magnetic Tracking System...," *IEEE Trans. Ind. Informat.*

ztangyitxiaang@gmail.com